QUENCH DYNAMICS OF FERMIONS IN ONE-DIMENSION

by

Ryan Cadigan

A Thesis

Presented to the Faculty of
Bucknell University
in Partial Fulfillment of the Requirements for the Degree of
Bachelor of Science with Honors in Physics & Astronomy

October 22, 2017

Approved: _____

Dr. Deepak Iyer
Thesis Advisor

_____

Dr. Michele Thornley
Chair, Department of Physics & Astronomy

Acknowledgments

This work has been supported by Bucknell's Program for Undergraduate Research, the Department of Physics and Astronomy, and the Linux Computer Cluster.

Thank you to the thesis defense committee, for your patience and consideration.
To Marty Ligare, for being my second reader.
To the Math Department, for granting this work my Culminating Experience.
To the Physics & Astronomy Department, for the knowledge, hospitality, and pizza.
To my dogs, Shadow and Scout, for the emotional support.
To my adviser, Deepak Iyer, for your patience, guidance, and, above all, your time.
To my family, for the valuable opportunities you provide and the invaluable faith you have in me.

Contents

Abstract

A variety of recent studies have shed light on the far from equilibrium behavior of quantum systems. Research suggests that this away from equilibrium approach may lead to the realization of unfamiliar dynamical quantum states. For instance, we see ballistic transport at finite temperature, an absence of thermalization, and development of long-range entanglement from initially uncorrelated states.

It has been shown that in some cases a time-evolving quantum state is equivalent to the ground state of an "emergent" Hamiltonian where the time enters as a parameter. This mapping gives us insight into the nature of correlations between particles. For high temperatures, we expect no long-range correlations to develop. However, the emergent model demonstrates that the time-evolved state can be realized as a low energy eigenstate, which naturally possesses long-range correlations.

Here, we study the dynamical behavior of both noninteracting and interacting particles in a one-dimensional lattice under various conditions. As the system undergoes time evolution, we look at the distribution of particles as well as correlations between particles in the system. We then compare the actual time-evolving state of the system to the ground state of the emergent Hamiltonian to study how long this description is valid. We generally expect that the description is valid in a given region as long as the boundary effects do not propagate into the region.

We first verify and reproduce results in the literature (see Vidmar *et al.* [1]). We proceed to study the effect of interaction strength in a particular interacting model that shows both ballistic and diffusive transport. We then apply this formalism to calculate infinite temperature dynamics of a noninteracting system. Interestingly, this system also develops long-range correlations over time in spite of starting out from an infinite temperature state.

Chapter 1

Introduction

This thesis examines the equilibration dynamics of one-dimensional interacting and noninteracting quantum systems. These systems are taken far from equilibrium initially and released. These types of systems yield interesting phenomena as they evolve. This behavior cannot be understood through the standard statistical mechanics framework used to describe equilibrium and near equilibrium dynamics.

Here, I explain the difficulties in studying these types of nonequilibrium systems and why these results are of interest. The following two chapters provide a description of the underlying physics of and methods used in studying these systems. I proceed to explain the characteristics of each of the systems and discuss the results.

I also discuss the notion of integrability and methods involved in studying integrable systems. Intregrability is intimately related to thermal equilibration (or the absence of it), a behavior which is characterized by the long-time averages of physical observables being defined by the Gibbs ensemble and the energy eigenvalues of the system. Experimentally, most systems are shown to achieve thermal equilibrium, but notably, integrable or near integrable systems do not [2]. The systems we simulate can be experimentally studied in the context of domain wall quenches involving ultracold atoms and sudden expansion of quantum gases.

1.1 Nonequilibrium Physics

Statistical mechanics is used to generate emergent behavior of systems based on their constituent components. However, this formalism only applies to quantum systems near equilibrium. There is no such framework to describe the behavior of quantum systems driven far from equilibrium [3]. Interacting systems are typically nonlinear, meaning the response to some perturbation is not proportional to the magnitude of that perturbation [4]. Integrable interacting systems (and other classes of systems which show "many-body localization") that have an extensive number of local conserved quantities, produce out of equilibrium states, which are not described in this regime [5]. They are often non-ergodic; they do not sample from the entire spectrum of available states. This means that there are some possible states in which the system could be, theoretically, but are not accessible from its current state. This violates the fundamental assumption of statistical mechanics, which states that for an isolated system in equilibrium, all microstates are equally probable [6]. The problems we consider shed light on systems whose behavior is not established in the context of traditional statistical mechanics.

1.1.1 Quench Dynamics

We model quantum systems taken far from equilibrium on a one-dimensional lattice. The dynamics of these systems are described in terms of particles hopping among lattice sites. These models exhibit domain wall melting phenomena, which is seen in Figure 1.1. A domain wall characterizes the initial setup of a system. The particles start uniformly occupying a particular region of the lattice. Our systems begin to relax to equilibrium immediately after the removal of the confining potential. This is known as a quantum "quench." As a system equilibrates, the domain wall "melts" into the initially unoccupied half of the lattice, as particles hop into this region.

The Hamiltonian of a system characterizes its energy and governs its evolution over time. In this case, we take the Hamiltonian to be time-independent. To find the state of the system at a given time t, we first represent the initial state $|\psi_0\rangle$ in terms of the energy eigenstates, the quantized states of definite energy. In this context, an eigenstate is an eigenvector of the Hamiltonian, which has a corresponding energy eigenvalue. See Appendix A for information regarding eigenvectors and

eigenvalues. These eigenstates form an orthonormal basis, which means we can use the completeness relation to write

$$|\psi_0\rangle = \sum_n \langle E_n|\psi_0\rangle |E_n\rangle. \tag{1.1}$$

The completeness relation is described in further detail in Appendix B. Letting $\hbar = 1$, the evolution of energy eigenstate $|E_n\rangle$ is given by the propagator $e^{-iE_n t}$. Applying this to all energy eigenstates, we arrive at an expression for the time evolved state given by,

$$|\psi(t)\rangle = \sum_n e^{-iE_n t}\langle E_n|\psi_0\rangle |E_n\rangle. \tag{1.2}$$

See *Quantum Mechanics: A Paradigms Approach*, Chapter 2, by David McIntyre for further details [7].

To quench a system is to suddenly change the Hamiltonian [8]. The quench initiates dynamics because, after the quench is performed, the system is no longer in an energy eigenstate under the new Hamiltonian, but rather is in a linear combination of such states. It is important to distinguish quench processes from adiabatic processes. In the adiabatic case, the change is sufficiently slow such that the system remains in an eigenstate throughout the entire process [6].

1.1.2 Thermalization

Despite the extensive number of possible equilibria quantum systems can achieve, the vast majority of these systems relax to thermal equilibrium [8]. This equilibrium process is known as thermalization. It was long conjectured that thermalization is a consequence of the typical properties of individual eigenstates [9, 10] and this was confirmed in 2007, by Rigol *et al.* [11]. As a result, for a many-body eigenstate thermalization situation, thermal averages can be calculated given knowledge of the eigenstate and a few properties of the initial state, typically the energy. The average value of observable $\hat{O}$ after a sufficiently long time is given by,

$$O_T = \lim_{T\to\infty} \int_0^T \frac{\langle O(t)\rangle}{T} dt, \tag{1.3}$$

which is equivalent to

$$O_T = \mathrm{Tr}[Oe^{-\beta\hat{H}}] \tag{1.4}$$

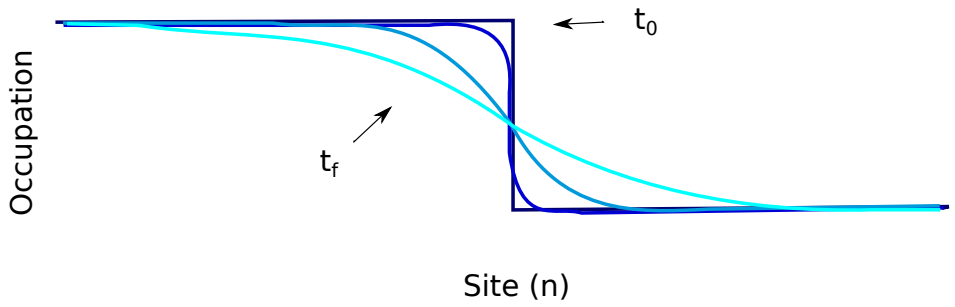

Figure 1.1: Domain wall melting schematic. Initially, at time t_0, particles start uniformly occupying the left half of the lattice. This domain wall setup is an eigenstate of the initial Hamiltonian. After the quench, the Hamiltonian is changed such that the initial setup is no longer an eigenstate. As the system evolves, the domain wall "melts" into the right half of the lattice. As described by the cyan curve at time t_f, the occupancy distribution becomes more evenly distributed along the lattice as particles hop into this initially unoccupied region.

where β is inverse temperature [12].

The Eigenstate Thermalization Hypothesis (ETH) [9, 10] looks to explicitly establish the means by which a system reaches thermal equilibrium. There are various conjectures pertaining to the ETH. For example, it is suspected that local physical observables correspond to eigenstates that are essentially indistinguishable from thermal states of the same average value [12]. For information on the ETH, see D'Alessio *et al.* [13].

One class of systems, known as integrable quantum systems, typically do not thermalize. Integrability is discussed further in Section 2.2. Integrable systems are characterized by their many locally conserved quantities [14]. Given the numerous conserved quantities, there are many local operators, which commute with the Hamiltonian and each other. It follows that the system cannot range over the entire spectrum of states corresponding to thermal equilibrium [12, 13]. The definition and significance of commutation relations are given in Appendix B.

The ETH can be extended to integrable quantum systems. The system still is expected to relax to some equilibrium as entropy is maximized. The generalized Gibbs ensemble (GGE) is used to describe the long-time average of physical observ-

ables in integrable quantum systems [15]. The corresponding observables of these systems relax to stationary values as the system thermalizes, but instead of a single temperature, there are several parameters. For integrable models, it has been shown that the stationary values of local observables are given by their expectation values with respect to a single eigenstate of the initial Hamiltonian [16]. This means that the information about initial conditions is contained in the state throughout its evolution, whereas an ergodic system loses this information over time. Experimentally, however, all systems have been shown to eventually relax to thermal equilibrium due to nonintegrable processes [2]. Despite this, experiments have also confirmed systems theoretically expected to relax to a state described by a GGE, such as a degenerate Bose gas in one-dimension [17].

1.1.3 Transport Phenomena

A particularly applicable aspect of far from equilibrium quantum systems is the insight their dynamics produces into currents and other transport phenomena. In the types of systems we observe, current is not restricted to being merely a flow of particles, as it is typically in classical physics. A "current" can refer to the movement of physical properties, including spin, charge, or energy. Some systems, such as the Hubbard model, yield spin-charge separation, in which case the physical properties become delocalized from particles (see Section 5.2).

The currents we observe are characterized as either ballistic or diffusive. Ballistic currents spread at a fixed velocity throughout the lattice. Most zero temperature systems we model exhibit ballistic transport. That is, following the quench, the particles spread throughout the lattice at a fixed rate. It is conjectured that, in fact, all integrable models demonstrate ballistic transport [18] as a consequence of exhibiting nonergodicity and conserved energy [19] in some regime. Diffusive currents slow down over time. In some cases, the spread is bounded. That is, the current still propagates for all time, but the transport does not extend beyond a particular region of the lattice in finite time. Diffusive transport occurs in the gapped t-V model, which is discussed in Section 5.1.2.

1.2 Ultracold Atom Experiments

Ultracold atomic gases are particularly useful systems in which to experimentally study quantum equilibration dynamics. Experiments involving ultracold gases often consist of optical lattices. These lattices are constructed and cooled through interfering laser beams [20]. This process sheds light on nonlinear wave dynamics and strongly correlated quantum phases with periodic potentials [20]. An external magnetic field present on a Fermi gas, for example, can be tuned to analyze the effects of the strength of interactions between particles [21].

The systems we study start in a domain wall setup, discussed in Section 4.1.1 for noninteracting models. In a domain wall, particles uniformly occupy a region of the lattice. To engineer this setup experimentally, all particles' spins initially align in the direction of a strong, applied magnetic field. A π-pulse is then applied to a particular region, which flips the spins via the straightforward classical interaction of spins with magnetic fields. Such experimental setups are described further by Kirilyuk *et al.* [22]. Interactions among particles are tuned through Feshbach resonances [23]. These resonances involve a change in a magnetic field, which affects the interactions between atoms confined to the lattice. Techniques have been developed to control interactions between neighboring particles [24]. Duan *et al.* have shown that spin interactions of the particles can be controlled by adjusting the intensity, frequency, and polarization of the trapping light.

1.3 An Emergent Approach to Quantum Dynamics

Particle interactions provide information about currents and other transport phenomena in the lattice. Given a particle with a dynamical quantity such as spin or charge, we can move to a reference frame in which it is at rest [1]. Thus, it can be modeled as a steady state solution of some other system. One can generate an emergent Hamiltonian, such that it contains a particular eigenstate which can be used to model the state of the system over time, as has been done by Vidmar *et al.* [1]. Only one eigenstate needs to be obtained in this effective approach rather than a full diagonalization and sum over an entire spectrum as necessary in the exact

time-evolved solution.

1.3.1 Interacting vs. Noninteracting Systems

In noninteracting systems, the particles do not interact, meaning the multi-particle state can be written as a direct product of single particle states. To do this explicitly, we use Slater determinants, a method which is discussed in Section 3.3. It follows that the evolution of the N particle system is equivalent to the composition of the evolution of a single particle system for each of the N particles in the lattice. With this simplification, the noninteracting systems we consider can be solved analytically.

Interacting systems involve an interaction energy in addition to the hopping kinetic energy. That is, the behavior of a certain particle depends on the positions of the other particles relative to it. A notable example of an interacting system is the Heisenberg XXZ spin chain, which is discussed further in Section 2.3.2. As a result of this interaction energy, the state cannot be written in the form of a Slater determinant. The exact time-evolved solution therefore cannot be solved analytically. These systems require full diagonalization of the Hamiltonian to generate the eigenstate spectrum used in the calculations of observables. Further, the Hilbert space grows exponentially with increasing system size, whereas the space for noninteracting systems grows linearly. We are greatly limited on the size of the interacting systems we study. These calculations are discussed further in Chapter 3.

1.4 Outline

The rest of this thesis is organized as follows. In Chapter 2, I provide further motivation for the approach to this work including an overview of mathematical formalism, techniques used in our models, and other experimental applications. In Chapter 3, I discuss numerical procedures used to implement and generate results for the systems we observe. Our work for noninteracting models in presented in Chapter 4. The chapter begins with the zero temperature case. I outline the effective approach and present the results for the effective and exact solutions. The latter part of the chapter includes our work for nonzero temperatures. I discuss the differences in these systems and present our work for the infinite temperature case. The chapter concludes with

a discussion of the difficulties in the study of finite temperature systems. Chapter 5 contains our work on interacting models. I describe the physics of the systems we consider as well as further numerical methods used to model them. The chapter also includes a discussion on finite temperature interacting systems. Chapter 6 concludes with a discussion and summary of our work.

Chapter 2

Background

In this chapter, I first present an overview of the underlying mathematical framework in our models. This includes a discussion of second quantization and its application to the single particle correlations we calculate. I also provide an overview of the types of systems we observe and the various methods used to study them. The chapter concludes with a description of finite temperature quench dynamics.

2.1 Second Quantization

Second quantization formalism describes many-body quantum systems in Fock space, which is discussed below. This formulation is generated through an algebra of ladder operators, which effectively create or destroy a particle at a given site. In this context, we refer to these ladder operators as creation and annihilation operators. For further reference, see Altland, Simons,"*Condensed Matter Field Theory*", Chapter 2 [25].

2.1.1 Fock Space

The dynamics of classical systems are entirely deterministic. Classical particles are distinguishable from one another, and each particle's evolution in phase space is

readily solvable [26]. Quantum systems do not behave this way. Quantum particles are indistinguishable from one another; swapping the positions of two particles in a quantum system does not change the state of the system. Quantum states are written in Fock space to account for this indistinguishability. We study spinless (or spin-polarized) fermionic systems, which can only be occupied by at most 1 particle per site, as a result of the Pauli-exclusion principle [7].

2.1.2 Particle Creation and Annihilation Operators

In Fock space, states are generated by creation and annihilation operators. Further, these operators govern the evolution of Fock states. These operators effectively act on the state to add or subtract a particle at a particular site. More specifically, the creation operator $\hat{c}_j^\dagger$ increases the occupation number at site j by 1. The annihilation operator $\hat{c}_j$ decreases the occupation number at site j by 1. If there is no particle at site j, the annihilator is then acting on the vacuum $|0\rangle$, which kills the state. The wavefunction of fermions is antisymmetric. This property gives rise to the Pauli exclusion principle and the antisymmetric commutation relations. That is,

$$\{\hat{c}_i, \hat{c}_j^\dagger\} = \hat{c}_i\hat{c}_j^\dagger + \hat{c}_j^\dagger\hat{c}_i = \delta_{ij} \tag{2.1}$$

$$\{\hat{c}_i, \hat{c}_j\} = \{\hat{c}_i^\dagger, \hat{c}_j^\dagger\} = 0 \tag{2.2}$$

and thus,

$$\hat{c}_i^\dagger\hat{c}_j = -\hat{c}_i\hat{c}_j^\dagger \qquad (i \neq j). \tag{2.3}$$

The Fock basis states are represented in terms of creation operators acting on vacuum state $|0\rangle$. Each basis state is a single particle at a particular site,

$$|x_j\rangle = \hat{c}_{x_j}^\dagger|0\rangle. \tag{2.4}$$

These basis states are orthonormal and span position space (see Appendix B). It follows that the occupancy distribution at any given time corresponds to a particular set of basis states. The time-evolving state may therefore also be represented in terms of creation operators acting on the vacuum state. In a system of N particles, the state at a given time is of the form

$$|\{x_j\}\rangle = \prod_{j=1}^{N} \hat{c}_{x_j}^\dagger|0\rangle, \tag{2.5}$$

where $\{x_j\}$ is the set of occupied lattice sites.

Particles hop among lattice sites as the system equilibrates. These dynamics are governed by the Hamiltonian of the system, as seen in Section 1.1.1. This evolution is described via hops written in terms of creation and annihilation operators. The action of $\hat{c}_i^\dagger \hat{c}_j$ on a particular Fock state, effectively moves a particle from site j to site i. We are interested in the expectation values of these single particle correlations $\langle \hat{c}_i^\dagger \hat{c}_j \rangle$. Single particle correlation pair calculations are discussed further in Section 3.2.

2.1.3 Correlations and Long-Range Entanglement

Spatial correlations between particles are essentially a measure of long-range entanglement. Given the connection between classical thermodynamics and information theoretical quantities such as entropy, it has been conjectured that such entanglement may have a deeper influence on quantum thermodynamics that has yet to be fully understood [27]. These functions are expressed in terms of creator-annihilator pairs. The expectation value of correlation function $\langle \hat{c}_i^\dagger \hat{c}_j \rangle$ measures the entanglement between a particle at site i and j. When $\hat{c}^\dagger$ and $\hat{c}$ act on the same site, the pair is known as the density operator, denoted,

$$\hat{n}_j \equiv \hat{c}_j^\dagger \hat{c}_j. \tag{2.6}$$

Density operator $\hat{n}_j$ measures the occupancy at site j.

As will be seen in Chapter 3, the data for the systems we observe are contained in time-evolved correlation matrices. Each element of a correlation matrix describes the expected value of a particular correlator pair, i.e. the entanglement between the particles at the given sites. We typically consider the developing correlations with respect to a fixed site, which corresponds to a particular row of a correlation matrix. The diagonal elements of a correlation matrix describe the occupancy distribution of the system at a given time. These are the two quantities we highlight to understand a system's dynamics. Graphical single particle correlations and occupancy distributions results for the systems we observe are reported in Chapters 4 and 5.

2.2 Methodology

We study integrable models, which can be solved exactly, at least insofar as their equilibrium behavior is concerned. In addition to the methods used to study the systems we observe, and nonequilibrium quantum problems in general, this section explains specific techniques this property allows us to utilize. First, it is necessary to explicitly define integrability in a quantum system. Given the discretization of levels in quantum mechanical systems, we can work easily in Hilbert spaces of finite dimensions. The eigenstate observables of these spaces can be assigned a particular quantum number, ranging over a finite set of values. The number of degrees of freedom in a quantum system is typically the number of dimensions of its Hilbert space. The number of degrees of freedom in a classical system is the phase space dimensionality required to fully describe the state of the system. These phase space variables range over a continuous set of values. Given the infinite number of possible values these variables can take on in contrast with the finite set over which variables of quantum systems range, there is no correspondence between classical and quantum integrability [14].

2.2.1 Tight Binding Approximation

To model real systems by such integrable systems, we apply a tight binding approximation. The tight binding method is used to calculate electron band structures in a lattice [28]. The method only models one electron but can be used to generate a basis for many-body problems [29]. In this approximation, the energy eigenstates are written in terms of an atomic-like basis set, to effectively replace the exact Hamiltonian with a parametrized Hamiltonian matrix [29].

Wannier states span a useful basis for representing theory of interactions in this approximation. Here, I explain and define these states as established in Altland, Simons "*Condensed Matter Field Theory*", Chapter 2 [25]. Consider an electronic lattice in which sites are separated by a distance larger than the Bohr radius of valence electron bands. In such a system, the wavefunctions are "tightly bound" to the lattice sites. To describe the interactions between particles, we expand the Hamiltonian in a local basis that reflects the atomic orbital states at each site. This

representation is expressed in a basis of Wannier states defined,

$$|\psi_{\boldsymbol{R}_n}\rangle \equiv \frac{1}{\sqrt{N}} \sum_{\boldsymbol{k}}^{BZ} e^{-i\boldsymbol{k}\cdot\boldsymbol{R}} |\psi_{\boldsymbol{k}_n}\rangle, \quad |\psi_{\boldsymbol{k}_n}\rangle \equiv \frac{1}{\sqrt{N}} \sum_{\boldsymbol{R}}^{BZ} e^{-i\boldsymbol{k}\cdot\boldsymbol{R}} |\psi_{\boldsymbol{R}_n}\rangle, \tag{2.7}$$

where $\boldsymbol{R}$ contains the coordinates of lattice sites and $\sum_{\boldsymbol{k}}^{BZ}$ is a sum over all momenta $\boldsymbol{k}$ in the first Brillouin zone [25].

Notice that the Wannier states form a basis for single particle systems. This is an orthonormal basis in Hilbert space. So there is a unitary transformation between the real space and Wannier representation. These transformations are used to write the Hamiltonian in the basis of Wannier states. The resulting Hamiltonian explicitly describes the flow of charge current throughout the lattice via fermion hopping. In this representation, we can directly study the correlations developing between lattice sites and occupancy distribution over time. For further reference, see Altland, Simons "*Condensed Matter Field Theory*", Section 2.2 [25].

2.3 Models

The models we study are understood to produce notable phenomena [24, 30]. Even systems as seemingly simple as a one-dimensional lattice of spinless fermions at zero temperature exhibit unexplained behavior [1]. To model this behavior, we generate the time-evolved solution as described by the exact Hamiltonian and compare to the results of an effective approach, using the tight binding method seen in the previous section. This effective approach involves an emergent Hamiltonian, which describes the system's evolution over time (see Section 4.1.3).

2.3.1 Noninteracting

The systems we observe are physically realized as one-dimensional gases of fermions. Noninteracting fermionic models are often confined in harmonic traps [30, 31]. Vigonolo and Minguzzi demonstrated that occupancy distribution and single particle correla-

tions generated in a system confined as such demonstrated behavior describable via Fermi statistics [30].

2.3.2 t-V Model: Interacting Fermions

Many mapping techniques exist in one-dimensional systems, which demonstrate equivalence between models. As an example, consider Luttinger liquid theory. The Luttinger model is a notable application of interacting spinless fermions in one-dimension [32]. This model serves as a basis for describing one-dimensional Fermi gases, in general [33]. The model was solved exactly in 1965 by Mattis and Lieb [34]. Interestingly, Mattis and Lieb translated the problem into Bosonic language to describe the excitation spectrum [33].

A notable example of demonstrating interesting transport phenomena is the spin-1/2 XXZ chain. This models the behavior of a spin-1/2 Heisenberg ferromagnet [35]. The XXZ chain is exactly solvable via the Bethe ansatz, which solves integrable models, yet still provides unexplained phenomena [35]. The XXZ model can be mapped onto a spinless model for interacting systems, using a Jordan-Wigner transformation, which maps between spinless and spin-1/2 fermionic models [36]. This mapping generates the one-dimensional t-V model, which is the interacting system we simulate.

Chapter 3

Numerical Methods

In this chapter I discuss the techniques used to model the types of systems we observe. This includes a description of the underlying physics as well as implementation methods (i.e. numerical methods) used to generate quantities and results. I first compare the computational basis states used for noninteracting and interacting models and discuss the techniques used to generate each, given the different methods used to study their dynamics.

I proceed to explain methods used to calculate single particle correlation function expectation values. The physics behind this is straightforward, but it is valuable to make this algorithm as efficient as possible given the extensive number of times it is utilized in evolving the systems. For noninteracting systems we utilize bit-shift operators to efficiently operate on basis states. Interacting systems also employ binary strings, but require a more elaborate method given that time-evolved states are no longer direct products of single particle eigenstates. The following section discusses further methods of increasing efficiency of our simulations using parallelization, and their implementation.

3.1 Computational Basis States

For systems of noninteracting, spinless fermions, each site is in either of two states; namely, occupied or unoccupied. The presence or absence of a particle at a particular site is given by a 1 or 0, respectively. The computational basis states corresponding to Fock states are then naturally represented as binary strings.

3.1.1 Noninteracting Models

In noninteracting systems, these basis states are all possible occupancy distributions of one particle along the lattice, thus spanning the position space of a single particle system. The array of basis states then forms an identity matrix.

3.1.2 Interacting Models

States of interacting models cannot be written in the form of a Slater determinant. Instead, the set of basis states must consist of all possible arrangements of N particles along the length L lattice. This set is now of length $\binom{L}{N}$ instead of length L as it was for noninteracting models. Each basis state, however, is still represented as a length L binary string. Using Python's *itertools* module, we construct all possible arrangements of "$111\cdots000\cdots$", as seen in Listing 3.1. After generating these states, we return a list of strings starting with the binary string of the greatest numerical value. This is done to ensure the basis elements are sorted from lowest to highest energy.

Listing 3.1: Construct all possible distributions of particles along the lattice. The 'iterable' is a binary string of consisting of N 1's and $L-N$ 0's. The set of basis states is sorted by energy via reversed binary counting.

```
1 def basisArr(iterable):
2     '''
3     Construct computational basis states
4     '''
5     bases = itertools.permutations(iterable, L)
```

```
6       bases = list(set(bases))
7       bases = [''.join(state) for state in bases]
8       bases = sorted(bases)[::-1]
9       return bases
```

3.2 Calculating Expectation Values

For all the systems we study, almost all of the calculated observables involve a sum over single particle correlation functions, $\langle c_m^\dagger c_n \rangle$. These correlation functions are calculated with respect to the Fock bases, as discussed in Section 2.1.1. A crucial implementation in the code is the operation of these single particle correlators on a particular Fock basis and the resulting expectation value. The simulation run time depends greatly on this operation; it is vital that this method be as efficient as possible given the extensive number of times it is called.

3.2.1 Noninteracting Models

This implementation is given in Listing 3.2. We first check that there is indeed a particle at the annihilation site. Note that if there is no particle at this site, the function will return 0, as desired, regardless of the equivalence between the states after the operation. The operation (on the right-hand basis state) is performed via a bit-shift for the appropriate distance and direction. The sign of the difference between indices of the creation and annihilation sites indicates a left or right bit-shift.

Listing 3.2: Calculate single particle correlation expectation value between sites given 'cdag' and 'c' with respect to bases m (left) and n (right) for noninteracting system.

```
1  def expVal(basis_m, basis_n, cdag, c):
2      '''
3      Correlation function expectation value
4      '''
```

```
    check_c = float(basis_n[c])
    shift = c-cdag
    if shift >= 0:
        rbasis = int(basis_n, 2) << shift
    else:
        rbasis = int(basis_n, 2) >> -shift
    return check_c*float(int(basis_m, 2) == basis_n)
```

3.2.2 Interacting

Given that we can no longer use Slater determinants to construct eigenstates, we also cannot utilize the bit-shift operation method discussed in Section 3.2.1 to compute correlation function expectation values. As a substitute, to compute $\langle c_m^\dagger c_n \rangle$, we first generate a binary string of all 0's except at digits m and n, which are 1. The right hand basis is XOR-ed with this masking bitstring to move the 1 at the n digit to the m digit. The resulting string is filled from the left with 0's to ensure it is of the appropriate length, L. As before, we check the equivalence between the left basis and the transformed string and return its value as a float.

Listing 3.3: Calculate single particle correlation expectation value between sites given 'cdag' and 'c' with respect to bases m (left) and n (right) for interacting system.

```
def expVal(basis_m, basis_n, cdag, c):
    check_c = float(basis_n[c])
    if cdag != c:
        check_cdag = 1.0 - float(basis_n[cdag])
        mask = ['0']*L
        mask[cdag], mask[c] = '1', '1'
        mask = ''.join(mask)
        basis_n = bin(int(mask,2)^int(basis_n,2))[2:].zfill(L)
        return check_c*check_cdag*float(basis_m == basis_n)
    else:
        return check_c*float(basis_m == basis_n)
```

3.3 Slater Determinant

According to quantum indistinguishability, fermionic wavefunctions must be antisymmetric under particle exchange. The wavefunction of a single particle at site x_j in position space is written $\phi_m(x_j)$, where m indicates the particular energy eigenstate. For $N = 2$ fermions, the wavefunction is given by

$$\psi(x_1, x_2) = \frac{1}{\sqrt{2}}[\phi_1(x_1)\phi_2(x_2) - \phi_2(x_1)\phi_1(x_2)], \tag{3.1}$$

which is clearly antisymmetric, as described by the Pauli exclusion principle. This wavefunction can be written in the form

$$\psi(x_1, x_2) = \frac{1}{\sqrt{2!}} \begin{vmatrix} \phi_1(x_1) & \phi_2(x_1) \\ \phi_1(x_2) & \phi_2(x_2) \end{vmatrix} \tag{3.2}$$

and generalized to

$$\psi(x_1, x_2, \ldots, x_N) = \frac{1}{\sqrt{N!}} \begin{vmatrix} \phi_1(x_1) & \phi_2(x_1) & \cdots & \phi_N(x_1) \\ \phi_1(x_2) & \phi_2(x_2) & \cdots & \phi_N(x_2) \\ \vdots & \vdots & \ddots & \vdots \\ \phi_1(x_N) & \phi_2(x_N) & \cdots & \phi_N(x_N) \end{vmatrix} \tag{3.3}$$

for N fermions. State $|\{\phi_{q_j}\}\rangle$ is written explicitly in the form,

$$|\{\phi_{q_j}\}\rangle = \frac{1}{N!} \sum_{x_1,\ldots,x_N}^{L} \det \begin{vmatrix} \phi_{q_1}(x_1) & \cdots & \phi_{q_1}(x_N) \\ \vdots & \ddots & \vdots \\ \phi_{q_N}(x_1) & \cdots & \phi_{q_N}(x_N) \end{vmatrix} \prod_j^N c^\dagger_{x_j}|0\rangle \tag{3.4}$$

$$= \frac{1}{N!} \sum_{x_1,\ldots,x_N}^{L} \sum_p^{N!} (-1)^p \prod_j^N \phi_{q_j}(x_{p_j}) \prod_j^N c^\dagger_{x_j}|0\rangle. \tag{3.5}$$

$$\tag{3.6}$$

3.3.1 Zero Temperature

The domain wall setup is the lowest energy distribution of N particles for our choice of initial Hamiltonian. We model the exact time-evolved state of the system as the ground state of the emergent Hamiltonian derived in Chapter 4. To obtain the ground state, we diagonalize the emergent Hamiltonian and select the N lowest energy eigenstates. After obtaining the N lowest energy eigenstates, we construct the emergent Hamiltonian ground state using this method.

3.3.2 Infinite Temperature

In the zero temperature model, it was straightforward to determine the emergent Hamiltonian eigenstate used to model the exact solution over time. The particular set of single particle eigenstates used to generate the multi-particle eigenstate clearly reflects the energy of the set up. The domain wall, for example, is the lowest energy set up, so we use the N lowest energy eigenstates to generate the time-evolved state.

For mixed states, this process is not as straightforward. The time-evolved state is now written as a mixture of eigenstates of the emergent Hamiltonian. Recall that the initial state was engineered to include only a particular subset of the eigenstates of the initial Hamiltonian. The time-evolved state is written in terms of emergent Hamiltonian eigenstates at the same indices at which the initial Hamiltonian eigenstates of nonzero probability in the mixed state appear.

3.4 Observables in Noninteracting Systems

3.4.1 Emergent Hamiltonian

We use the single particle eigenstate basis discussed in Section 3.1 to construct the emergent Hamiltonian. As seen in Equation 4.9, each entry of the emergent Hamiltonian is the sum of expectation values of correlation functions in terms of these basis states.

Noting the form of Equation 4.9, each entry of the emergent Hamiltonian matrix at any particular time is the sum of two constant terms with the second multiplied by the given time. Therefore, to minimize run time, these constant terms are computed prior to parallelization. After specifying initial conditions and the times at which to gather data, constructing the basis states, and calculating the constant terms in the emergent Hamiltonian, we are ready to construct our time-evolving correlation matrices in parallel over the given set of times.

The following method is described for a particular arbitrary time step. The full method therefore follows without loss of generality. For a given time, we first construct the emergent Hamiltonian. We initialize the emergent Hamiltonian to the array of constant terms which are not multiplied by the time. We then return the sum of this array and the second array of constants multiplied by the given time.

3.4.2 Emergent Eigenstate

From this emergent Hamiltonian, we construct the time-evolved state of the system. We first diagonalize the emergent Hamiltonian to obtain its energy eigenvalues and eigenstates. As discussed in Section 3.3, the state of the system corresponds to a set of N eigenstates. The binary string representing the initial state of the system indicates this particular set of eigenstates. To obtain them, we first construct a sorted list of the energy eigenvalues. Recall that for each initially occupied site in the lattice, we append the energy eigenvalue at the same index in the sorted eigenvalue list. In the domain wall set up, for example, we append the first N lowest energy eigenvalues to this list, given that the domain wall is the lowest energy state of the system. We now have the list of energies of the eigenstates corresponding to time-evolved state. Finally, we return a list of the corresponding eigenstates for each energy eigenvalue.

The time-evolved state of the system is entirely deterministic; the state at any given time can be calculated directly from the initial conditions. Therefore, to maximize the efficiency of our program, the density matrices for the exact solution and effective model for a set of times are computed in parallel.

3.4.3 Initial Conditions

Before parallelizing over the various time steps, we first compute the time-independent quantities. Naturally, the Hamiltonian $\hat{H}$ will always be calculated prior to parallelization for each of the interacting models.

However, before running the code in parallel, we must first specify the initial conditions of the system and the set of computational basis states. For systems of noninteracting, spinless fermions, each site is in either of two states; namely, occupied or unoccupied. The presence or absence of a particle at a particular site is given by a 1 or 0, respectively. To implement the initial conditions of the system, we build a binary string of length equal to the length of the lattice. In this case, number of particles is equal to half the length of the lattice, so the string will have an equal number of 1's and 0's. We also construct a list of indices of the sites which the particles initially occupy, which is needed for the analytical solution.

Given that the correlation matrices are Hermitian, we only need to apply Equations 4.5 and 4.10 to the upper triangles of these matrices. After constructing those regions, we simply set the lower triangles equal to their complex conjugates.

Chapter 4

Noninteracting Spinless Fermions

In this chapter, we consider noninteracting systems. As discussed in Section 3.3, in these systems, the only energy comes from particles hopping among lattice sites. We can therefore write states in terms of single particle eigenstates. Using this technique, we can generate results for exponentially larger noninteracting systems than for interacting systems in the same amount of time.

We also model noninteracting systems at nonzero temperature. The infinite temperature case we examine models transport phenomena, which have been observed in experimental domain wall quench problems [17, 22]. Interesting phenomena are apparent in all systems we study. In all cases, the system starts in an uncorrelated state. However, over time, we see correlations develop. These correlations suggest that quantum information and consequently entanglement is being dynamically generated as the system evolves.

4.1 Zero Temperature

The work presented in this section has been done previously by Vidmar *et al.* [1]. I have replicated results therein as a test for further work (see Section 4.2). The first system we consider consists of noninteracting particles at zero temperature. The system's dynamics can be effectively be described as the product of single particle

evolutions, as discussed in Sections 1.3.1 and 3.3. In a dynamical situation, when the system is evolving under the Hamiltonian, it reaches equilibrium through particles hopping among lattice sites. Given the lack of interactions between particles, all information is retained in the single particle eigenstates at all times. These single particle eigenstates are momentum eigenstates. It follows that the system never achieves thermal equilibrium.

4.1.1 Setup

The particles start in a domain wall state along a one-dimensional lattice, as shown in Figure 1.1. This setup is an eigenstate of an initial Hamiltonian, which is defined

$$\hat{P} = \sum_{j=} j\hat{h}_j \tag{4.1}$$

$$= \sum_{j} j\left[-J(\hat{c}_j^\dagger \hat{c}_{j+1} + \hat{c}_{j+1}^\dagger \hat{c}_j)\right]. \tag{4.2}$$

The system we consider is half-filled indexed $-N$ to N. As a result, initial Hamiltonian $\hat{P}$ generates a tilted linear potential, with the leftmost site being at the lowest energy. After the quench, the Hamiltonian changes such that the domain wall is no longer an eigenstate. The post-quench Hamiltonian is given by,

$$\hat{H} = \sum_{j} h_j \tag{4.3}$$

$$h_j = \sum_{j} -J(\hat{c}_j^\dagger \hat{c}_{j+1} + \hat{c}_{j+1}^\dagger \hat{c}_j). \tag{4.4}$$

This Hamiltonian eliminates the tilted potential, meaning particles are free to hop throughout the system. As the particles hop among lattice sites to achieve thermal equilibrium, the domain wall melts into a more even occupancy distribution, as seen in Figure 1.1.

4.1.2 Analytical results

This integrable, noninteracting system is solved analytically. The exact solution to the single particle correlation between site m and site n is given by [1],

$$C_{mn} = i^{n-m} \frac{t(J_m(2t)J_{n+1}(2t) - J_{m+1}(2t)J_n(2t))}{n-m}. \tag{4.5}$$

where J is a Bessel function of the first kind. Note that the occupancy of site m is described by C_{mm} and can be obtained as a limit.

The correlations with respect to the middle site are seen in Figure 4.1. As the system evolves, the correlations develop $1/n$ power-law relationships. These long-range correlations typically only occur in the lowest energy state [1]. This suggests there exists an emergent Hamiltonian, the ground state of which can be used to effectively model the exact time-evolved solution.

4.1.3 Emergent Hamiltonian

Recall that initial state $|\psi_0\rangle$ is an eigenstate of an initial local Hamiltonian, $\hat{P}$. We quench the system to initiate dynamics. At this time, $\hat{P}$ is changed to a new Hamiltonian, $\hat{H}$, of which $|\psi_0\rangle$ is no longer an eigenstate. Recall that the state of the system evolves unitarily as $|\psi(t)\rangle = e^{-i\hat{H}t}|\psi_0\rangle$.

The emergent Hamiltonian derivation proceeds as in Vidmar *et al.* [1]. Using identity $\hat{I} = e^{i\hat{H}t}e^{-i\hat{H}t}$ we define time-dependent operator $M(t)$:

$$\left(e^{-i\hat{H}t}\hat{P}e^{i\hat{H}t} - \lambda\right)|\psi(t)\rangle \equiv M(t)|\psi(t)\rangle = 0. \tag{4.6}$$

Expanding $M(t)$ using the Baker-Campbell-Hausdorff identity (see Appendix B), we see that in general it is highly non-local having arbitrarily high-order commutators of $\hat{H}$ and $\hat{P}$. However, a particularly interesting result occurs when the commutator of the local Hamiltonians obeys the relation

$$[\hat{H}, \hat{P}] = ia_0\hat{Q}, \tag{4.7}$$

where a_0 is some constant and $\hat{Q}$ is the current operator, which is a conserved quantity, given that the number of particles in the system is fixed. In this case, the higher

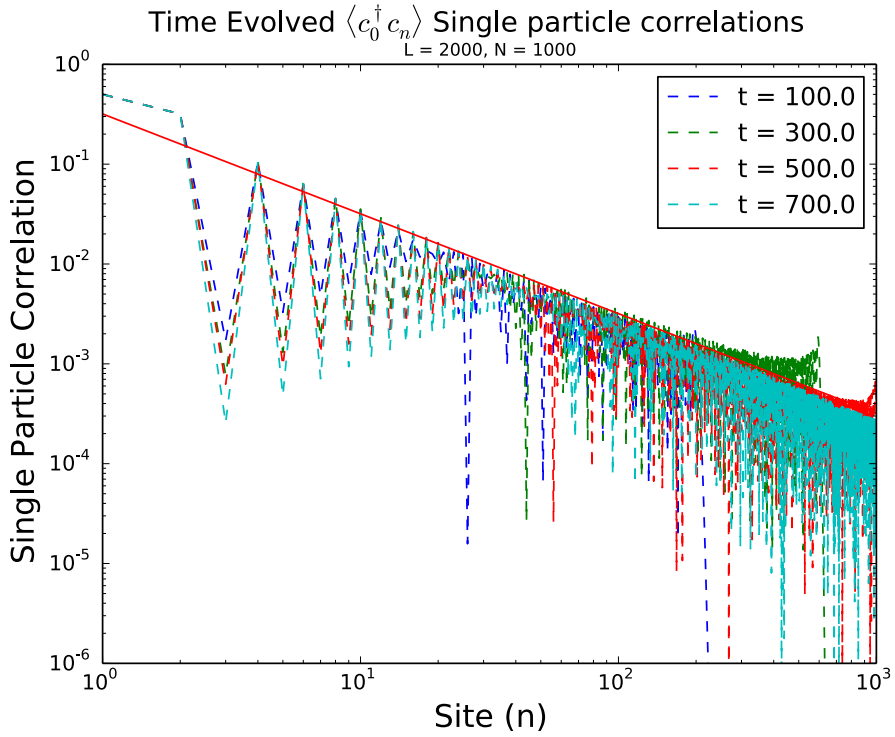

Figure 4.1: Analytical results at various times for noninteracting domain wall setup. These are single particle correlations for sites along the lattice each taken with respect to the midpoint. Over time, correlations develop $1/n$ power-law relations, as indicated by the straight, solid red line. This is most clearly seen towards the left edge of the plot. These types of correlations tend to only develop in the ground state, which suggests the existence of an emergent, time-dependent Hamiltonian that can be used to model the evolution. Note that the downward spikes are a result of finite system effects. These occur at odd indexed sites.

order terms of $\hat{M}(t)$ vanish and we are left with emergent Hamiltonian

$$\hat{\mathcal{H}}(t) \equiv \hat{P} + a_0 t \hat{Q} - \lambda. \tag{4.8}$$

The time-evolved state of the system is therefore an eigenstate of this Hamiltonian. For a domain wall initial set up, $|\psi(t)\rangle$ is the ground state of this Hamiltonian. The emergent Hamiltonian is given explicitly as

$$\hat{\mathcal{H}}(t) = \sum_j \left[j c_j^\dagger c_j - t(i\hat{c}_{j+1}^\dagger \hat{c}_j - i\hat{c}_j^\dagger \hat{c}_{j+1}) \right]. \tag{4.9}$$

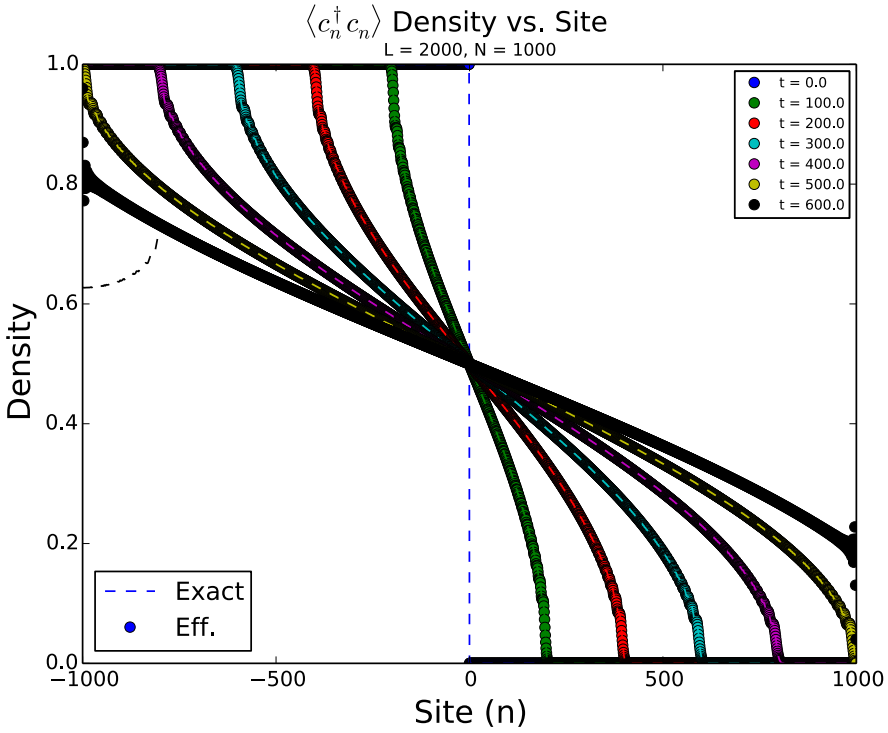

Figure 4.2: Occupancy distribution at various times for noninteracting domain wall setup at zero temperature. Initially particles uniformly occupy the left half of the lattice, as described by the curves at $t = 0$. As time evolves, the particles flow into the right half of the lattice. Exact analytical results are given by the dashed lines. Effective results are plotted as points and are consistent with the exact solution. However, in the final time plotted, $t = 600$, the solution curves begin to diverge. This breakdown occurs when particles begin to reach the right-hand boundary of the lattice.

This is the Hamiltonian that I use to calculate the time evolutions and compare to the exact solution.

At all times, we can diagonalize the emergent Hamiltonian and generate the corresponding set of emergent energy eigenstates, which describe the time-evolved state. The effective single particle correlation between site m and n is given by

$$C_{mn} = \sum_{j=1}^{N} \phi_{q_j}^*(m)\phi_{q_j}(n) \tag{4.10}$$

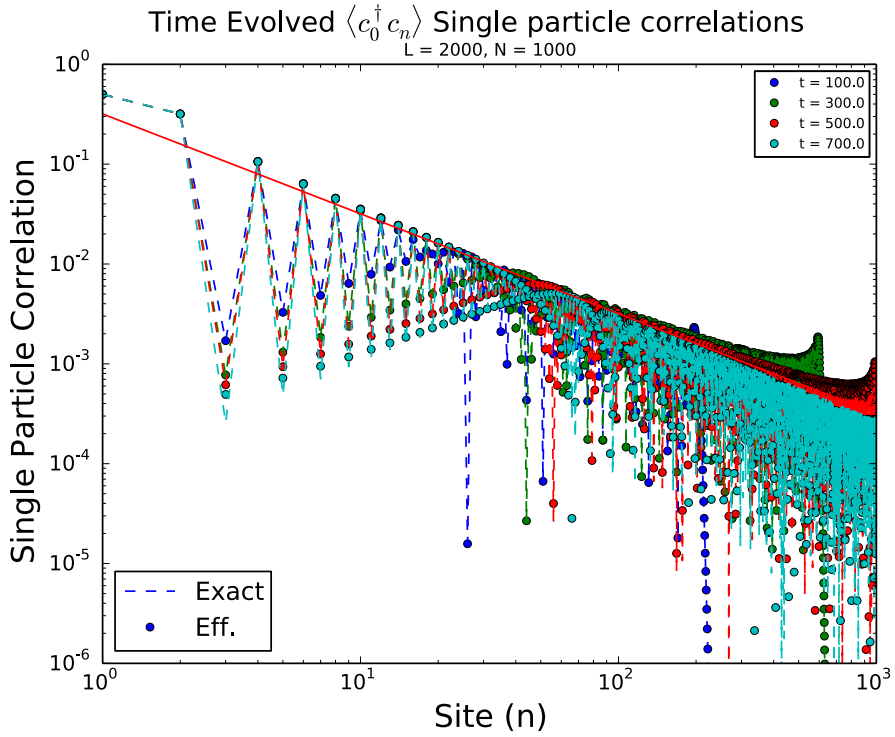

Figure 4.3: Single particle correlations $\langle \hat{c}_0^\dagger \hat{c}_n \rangle$ at various times for noninteracting domain wall setup. These are single particle correlations for sites along the lattice each taken with respect to the midpoint. Analytical results are given by the dashed lines. The effective model is consistent with analytical results. Over time, correlations develop $1/n$ power-law relations, as indicated by the straight, solid red line. This type of behavior is expected given that the left-hand domain wall is the lowest energy setup. Note that the downward spikes are a result of finite system effects. These occur at odd indexed sites.

where $\{\phi_{q_j}\}$ is the corresponding set of N single particle energy eigenstates.

4.1.4 Discussion

The occupancy distribution seen in Figure 4.2 exhibits the same domain wall melting seen in the schematic in Figure 1.1. The particles start uniformly occupying the left half of the lattice. As time evolves, the distribution becomes more uniform

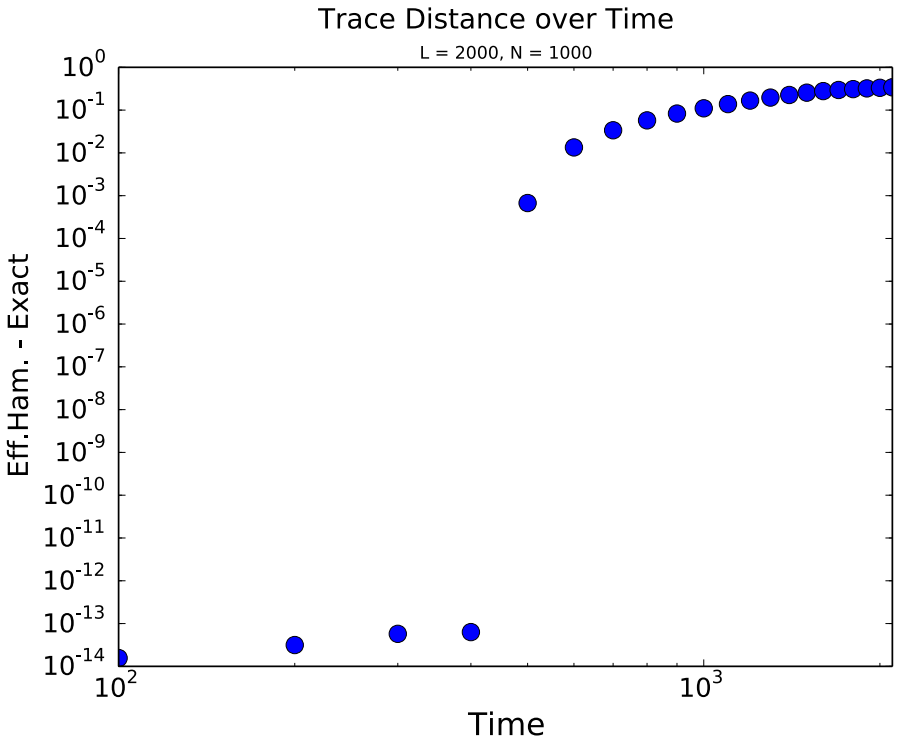

Figure 4.4: Trace distance between effective and exact correlation matrices at various times for noninteracting domain wall setup. The trace distance increases rapidly when $t/N \approx 0.4$, indicating the correlation matrices for each approach suddenly begin to differ. This disparity begins when particles reach the boundaries of the lattice.

throughout the system as the particles melt into the right half of the lattice.

We model the occupancy distribution and single particle correlations over time using both the exact and emergent eigenstate approaches. As can be determined from the plots, the emergent eigenstate approach is valid until $\frac{t}{N} \approx 0.4$. The breakdown of the effective model is due to finite system effects. The emergent Hamiltonian assumes open boundaries on the system and an infinite string of particles. Since the lattice consists of a finite number of sites, the two models will diverge when the particles begin to reach the boundaries of the system.

To quantitatively measure the error between the two models, we compute the trace distance between the correlation matrices corresponding to each approach.

This quantity is defined:

$$Tr(C_{\text{exact}}, C_{\text{eff.}}) = Tr(|C_{\text{exact}} - C_{\text{eff.}}|). \tag{4.11}$$

It can be shown that this is equivalent to

$$Tr(C_{\text{exact}}, C_{\text{eff.}}) = \frac{1}{2N} \sum_i |\lambda_i|, \tag{4.12}$$

where λ_i is an eigenvalue of $C_{\text{exact}} - C_{\text{eff.}}$. The number the trace distance returns describes the distance between the two arguments in matrix space. The trace distances shown in Figure 4.4 indicate the validity of the effective approach over time.

4.2 Infinite Temperature

We now introduce temperature into the system. Particularly interesting phenomena occur for nonzero temperatures in one-dimension. For instance, entropy kills all ordered phases in one-dimensional systems. At nonzero temperature, wavefunctions are expressed as mixed states. We start with a system at infinite temperature. This system describes the dynamics of a sudden expansion of quantum gas and other domain wall quench problems.

4.2.1 Mixed States

In the zero temperature models, the state of the system is written as a pure state. It starts as an eigenstate of the initial Hamiltonian and evolves as an eigenstate of a time-dependent emergent Hamiltonian. The state of a system at nonzero temperature is written as a mixed state. Instead of starting as a particular eigenstate of the initial Hamiltonian, the state is expressed using a density matrix, that allows us to express expectation values of operators as traces, in order to capture the averaging over different states that participate in the mixture with weighted probabilities.

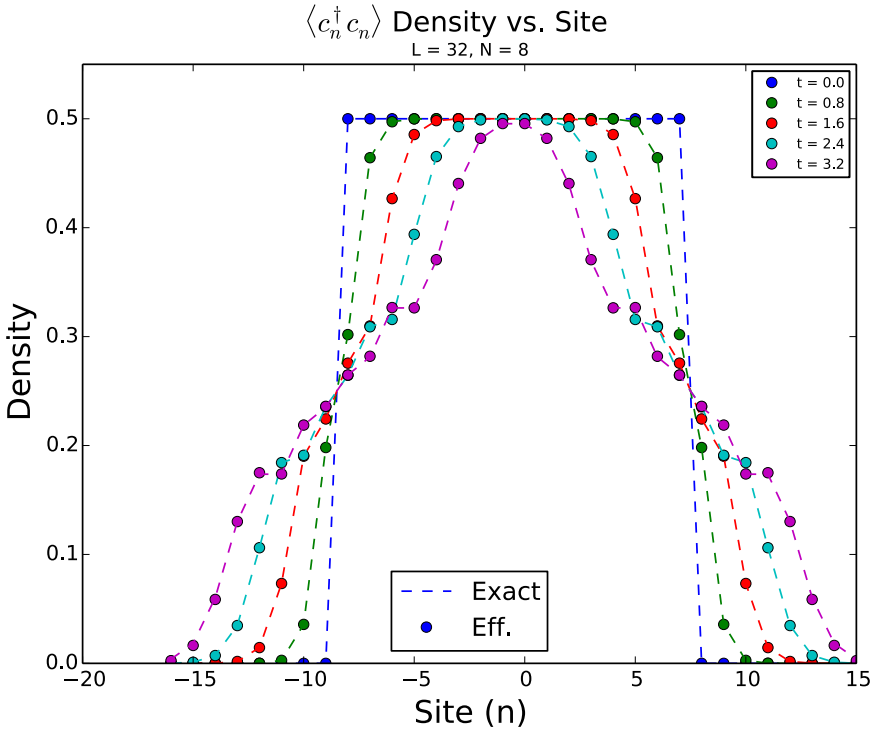

Figure 4.5: Occupancy distribution at various times for noninteracting system $J = 1.0, V = 1.2$ at infinite temperature. Particles start in a centered domain wall setup, the shape of which is clearly described by the distribution at time $t = 0$. Exact results are given by the dashed lines. A similar domain wall melting pattern occurs in this setup as in the zero temperature case, except on both sides of the domain wall. The initial state is engineered such that particles may only occupy the central region at time $t = 0$. For nonzero temperature, the system is described as a mixed state. For the initial setup, we require that any basis states in which particles occupy the fringes (regions outside the central half) of the lattice occur with probability 0. This yields the central domain wall initial setup previously discussed.

4.2.2 Initial Conditions

The only eigenstates of the initial Hamiltonian that occur with nonzero probability in the initial set up are ones in which the particles occupy the central half of the lattice with the fringes empty. We work out the infinite temperature case as a simple example. This set up describes the sudden expansion of a hot quantum gas.

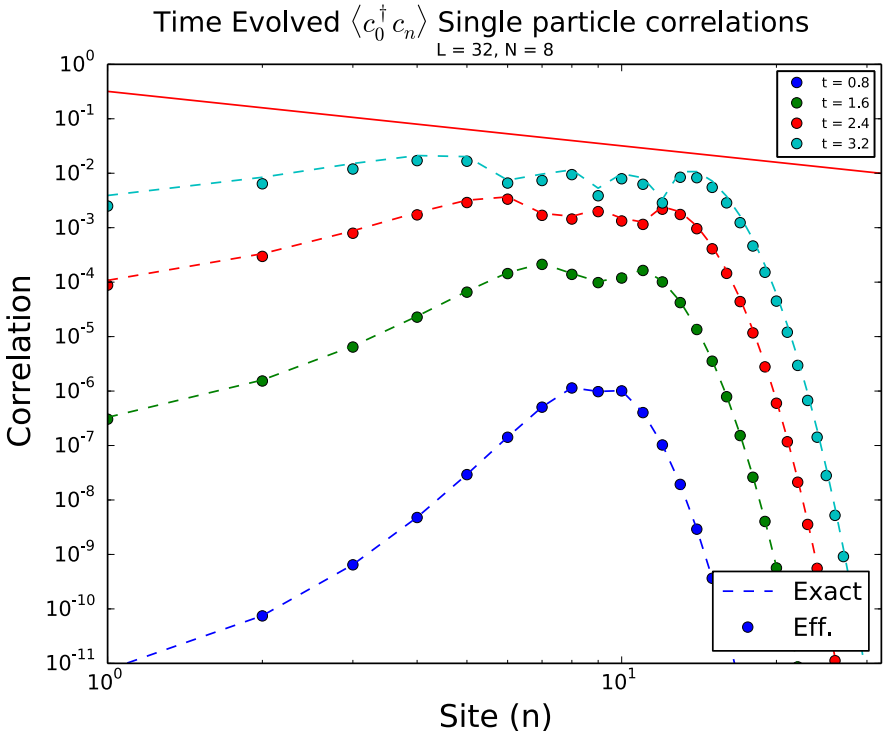

Figure 4.6: Midpoint correlations at various times for noninteracting system $J = 1.0, V = 1.2$ at infinite temperature, starting in a centered domain wall setup. These are single particle correlations for the right half of the lattice, each taken with respect to the midpoint of the system. Exact results are given by the dashed lines. The straight, solid red line gives power-law relationship $1/n$ for visual reference. The initial state is engineered such that particles may only occupy the central region at time $t = 0$. The system still develops power-law correlations over time. This is most clearly seen towards the left edge of the plot. Correlations are stronger and develop more quickly in this region given its closer proximity to the midpoint site. At the earliest time plotted, $t = 0.8$, the system is much less entangled compared to time $t = 3.2$, at which time the cyan curve is much closer to the $1/n$ line. We especially do not expect this behavior in this infinite temperature case. Firstly, the system begins in an uncorrelated state. Secondly, high temperature states have high energies, and these correlations typically only develop in low energy states.

The length of the lattice is now four times the number of particles in the system. The initial domain still however, occupies half of the lattice given that the system

is in a mixed state. As seen in Figure 4.5, the initial sites of nonzero density start at 0.5, rather than 1.0 as it was in the zero temperature set up. The occupancy distribution shown in Figure 4.5 exhibits a similar melting pattern over time as the left-hand domain wall set up at zero temperature. In this central domain wall setup, the melting occurs on both sides, since particles have room to hop.

The correlations with respect to the midpoint site ($n = 0$) for both approaches are shown in Figure 4.6. Notice that long-range power-law correlations still develop in the infinite temperature model. Results are only plotted at times for which the effective approach is a valid description. This means the particles have not yet reached the boundaries of the lattice, which is why the correlations drop off towards the right edge. Notice how the correlations towards the left edge alter the overall shape of the plot over time as the domain wall melts into fringes; the left half develops correlations much quicker than the right, as expected.

4.3 Finite Temperature

Although we do not have results for finite temperature, here we discuss the framework able to be used to study these types of systems. Consider a finite temperature system on a one-dimensional ring. With periodic boundary conditions, the system is translationally invariant. The density matrix is given by,

$$\hat{\rho} = \sum_{\{|\alpha\rangle\}} e^{-\beta E_\alpha} |\alpha\rangle\langle\alpha|. \tag{4.13}$$

Since the number of particles is conserved, there is no chemical potential. The relative weight of each eigenstate is governed by the energy in the canonical ensemble. The expectation value of an observable, $\hat{O}$ is given by,

$$\langle \hat{O} \rangle = \frac{Tr[\hat{p}\hat{O}]}{Tr[\hat{p}]}. \tag{4.14}$$

Recall that low energy eigenstates are long-range correlated states. With increased energy, the momentum of the eigenstates increases and therefore shortens the range of correlations. Since $\beta \propto \frac{1}{T}$, and T depends directly on thermal energy, β becomes a measure of correlation length.

The long-range correlations seen in the infinite temperature case are a particularly interesting result given that the system starts in an uncorrelated state. As the system approaches equilibrium, the correlations develop power-law relationships. The setup describes a hot quantum gas. However, for such high temperature systems, we do not expect any correlations to develop. In this case, the long-range correlations that form lay bare the unusual nature of nonequilibrium states.

Chapter 5

Interacting Models

Interacting systems include a potential energy among particles on the lattice. We look at nearest-neighbor interactions. For spinful models, these also include interactions between two particles on the same site. The interaction introduces transitions among energy eigenstates.

Interacting systems achieve equilibrium in the same way noninteracting systems do, i.e., hopping among lattice sites, however the particles are also influenced by scattering off their neighbors. In interacting systems the potential is nonzero. This means we can no longer use Slater determinants to write our time-evolved states. Since the particles now have influence on each other, we must explicitly account for the distribution when writing the state of the system. The computational basis states must now consist of all possible arrangements of particles along the lattice, rather than the set of single particle eigenstates as before.

Interactions in solid-state physics yield interesting phenomena. For example, in a Mott insulator, conductivity is suppressed as a result of strong electronic interactions [37]. In these insulators, controlling interactions as discussed in Section 1.2 enables comparison between the insulating and conducting regimes [38]. These phases produce other interesting phenomena, including superconductivity at high temperatures [39].

The Hubbard model also yields interesting physics. This system exhibits spin-

charge separation. These physical properties are no longer localized to a particle [40]. This poses a challenge to generating an effective model to describe the system's evolution, which is discussed further in Section 5.2.

5.1 t-V Model

Assuming an infinite on-site interaction strength (on equivalently a single spin species), we arrive at the t-V model with Hamiltonian written,

$$\hat{H}_{tV} = \sum_j h_j \tag{5.1}$$

$$h_j = \sum_j \left[-J(\hat{c}_j^\dagger \hat{c}_{j+1} + \hat{c}_{j+1}^\dagger \hat{c}_j) + V(\hat{n}_j - 1/2)(\hat{n}_{j+1} - 1/2) \right] \tag{5.2}$$

where V corresponds to the potential and J is the current density operator [41]. (In other contexts, 'J' is written as 't'; here we use 'J' to avoid confusion with time.) The t-V model captures the physics of a Mott insulator. It demonstrates both a conducting Luttinger liquid phase and Mott insulator phase [42]. It is also shown in Ref. [43] that this system can be mapped from the anisotropic spin-1/2 XXZ chain using the Jordan-Wigner transformation, a method to write spin creation and annihilation operators in terms of fermionic creation and annihilation operators [25].

This method we use to model the system was worked out previously by Vidmar *et al.* [1]. The initial Hamiltonian is given by,

$$\hat{P} = \sum_j j\hat{h}_j \tag{5.3}$$

$$= \sum_j j \left[-J(c_{j+1}^\dagger c_j + h.c.) + V(n_j - 1/2)(n_{j+1} - 1/2) \right] \tag{5.4}$$

which is the boost operator for current operator $\hat{Q}$ [19]. The boost operator effectively transforms the frame of reference to one moving with the flow of particles. This boost

operator satisfies $[\hat{H}, \hat{P}] = i\hat{Q}$ where $\hat{Q}$ is defined,

$$\hat{Q} = \sum_j \Bigg[iJ^2(c^\dagger_{j+2}c_j - c^\dagger_j c_{j+2}) \tag{5.5}$$

$$- iU\left((c^\dagger_{j+1}c_j - c^\dagger_j c_{j+1})(n_{j+2} - 1/2) + (c^\dagger_{j+2}c_{j+1} - c^\dagger_{j+1}c_{j+2})(n_j - 1/2)\right)\Bigg]. \tag{5.6}$$

We use a similar process as in Section 4.1.3 to define the emergent Hamiltonian. Starting from $\hat{P}$, we arrive at

$$\hat{\mathcal{H}}_{tV} = \hat{P} + t\hat{Q}. \tag{5.7}$$

5.1.1 Exact Diagonalization

The single particle time-dependent correlations cannot be solved analytically for interacting models, even though it is integrable and some equilibrium properties can be evaluated analytically. Constructing the time-evolved correlation matrix therefore requires a full diagonalization of the Hamiltonian. The exact correlations are given,

$$C_{mn} = \sum_{\alpha,\beta}\sum_{m,n} e^{it(E_\alpha - E_\beta)}\langle\alpha|\psi_0\rangle\langle\psi_0|\beta\rangle\alpha^*(m)\beta(n)\langle m|\hat{c}^\dagger_i\hat{c}_j|n\rangle \tag{5.8}$$

where $|\alpha\rangle$ and $|\beta\rangle$ denote energy eigenstates. We include a small potential on the leftmost site of the lattice to eliminate any degeneracy in energy levels [1].

We consider a half-filled lattice of length $L = 2N$ ranging from $j = -N$ to $j = N - 1$. After defining the initial conditions we construct the Hamiltonian of the system using Equation 5.1. We then diagonalize this matrix to get the corresponding energy eigenvalues and eigenstates. The remaining time-independent computations are the boost operator, $\hat{P}$, and current operator, $\hat{Q}$. We construct their corresponding matrices using Equations 5.4 and 5.6. According to the structure of the lattice, $\hat{P}$ ranges from $j = -N$ to $N - 2$ while $\hat{Q}$ ranges from $j = -N$ to $N - 3$.

The effective quantities are the first time-dependent calculations. The emergent Hamiltonian is constructed using Equation 5.7. We only need the time-evolving

ground state of this emergent Hamiltonian. We pick out the minimum eigenvalue and select the corresponding eigenvector to obtain the emergent ground state.

The effective correlation matrix is constructed with respect to the full $\binom{L}{N}$ set of eigenbases. Correlation between site i and j is given as,

$$C_{ij} = \sum_{m,n} \phi(m)\phi^*(n)\langle m|\hat{c}_i^\dagger \hat{c}_j|n\rangle \tag{5.9}$$

where ϕ is the appropriate eigenstate of the emergent Hamiltonian. As discussed in Section 2.1.1, the time-evolved ground state is represented in terms of this Fock basis. So each of the entries in the eigenstate provides the weight of the corresponding Fock state. We use Equation 5.9 to generate the effective correlation matrix.

The only time dependent quantity in the exact solution arises in the construction of the correlation matrix. These are then used to construct the time-independent quantities within the exact correlation matrix. Each entry of this matrix requires two sums over the $\binom{L}{N}$ energy eigenvalues and eigenstates. Recall that the energy eigenstates are overlapped with the initial state, $|\psi_0\rangle$, with respect to the Fock basis. Similarly, the correlation functions act directly on the Fock states and thus, require a weight given by the corresponding coefficients of the left and right eigenstates. The remaining calculation for a particular entry of the correlation matrix and pair of eigenstates is the time-dependent exponential factor, as shown in Equation 5.8. The results are plotted in Figure 5.1.

5.1.2 Gapped model

In the infinitely long limit, the spectrum of eigenstates is continuous. This means that for any amount of energy introduced into it, the energy will be transported throughout the lattice. Finite-region disturbances on the lattice do not remain localized to a particular section. In finite systems, the eigenstate spectrum is discrete, producing a separation between the ground and first excited states.

This energy gap will occur also in infinite systems if $V/J > 2$. In this case, the eigenstate spectrum is discretely infinite, with nonzero energy gap between the ground and first excited state. So it is possible to introduce a sufficiently small amount of energy, such that the energy remains localized to the region in which it

is introduced. The gapped model is expected to show diffusive or slow transport compared to the gapless model, which shows ballistic transport.

5.1.3 Results

The quenched domain wall for the t-V model exhibits a similar melting pattern to that seen in Section 4.1.4. The occupancy distribution over time for the gapped model is seen in Figure 5.2. The gapped model exhibits a similar melting pattern to the previous case, however, transport along the lattice is now diffusive. The occupancy distribution maintains its initial shape for longer times than in the ballistic transport case.

5.2 Hubbard Model

Although we do not have results for the Hubbard model, it is a natural extension of our work. Here we discuss the physical properties of this model and results found in previous literature. As seen in previous models, the charge current moves with some velocity. We can move to a frame of reference in which the charge is at rest. Therefore, we can describe the system as an eigenstate of another system. In the fermion models we've seen, there is an operator which carries out this Lorentz boost. The Hubbard model, however, has spin-charge separation, meaning its spin and charge currents are free to flow through the lattice independently at different speeds. Given this separation, the system is not Lorentz invariant.

The energy of the system is described

$$\hat{H} = \sum_{\sigma,j} \hat{h}_{\sigma,j} \tag{5.10}$$

$$= \sum_{j=-N}^{N-2} \Big[-J(c^{\dagger}_{\uparrow,j+1} c_{\uparrow,j} + h.c.) + U(n_{\uparrow,j} - 1/2)(n_{\downarrow,j} - 1/2) + (\uparrow \rightarrow \downarrow) \Big] \tag{5.11}$$

where

$$\hat{h}_{\uparrow,j} = -J(c^{\dagger}_{\uparrow,j+1} c_{\uparrow,j} + h.c.) + U(n_{\uparrow,j} - 1/2)(n_{\downarrow,j} - 1/2). \tag{5.12}$$

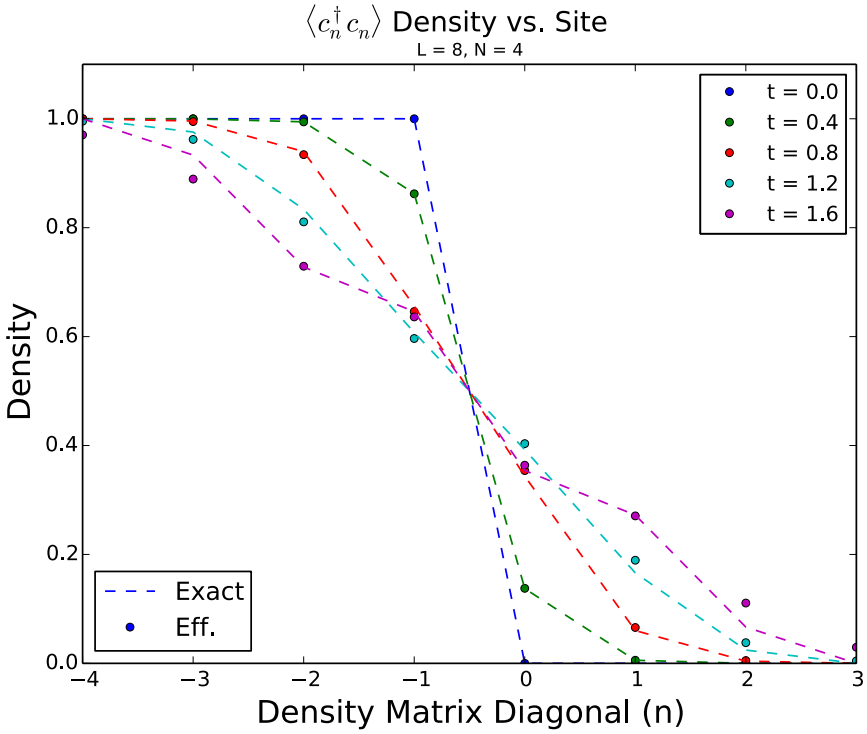

Figure 5.1: Occupancy distribution at various times for t-V model, domain wall setup for $J = 1.0, V = 1.5$. Initially particles uniformly occupy the left half of the lattice, as described by the curves at $t = 0$. Exact results are given by the dashed lines. Effective results are plotted as points and are consistent with the exact solution. Exhibits similar melting pattern as seen in the noninteracting domain wall at zero temperature.

The first term in the Hamiltonian corresponds to the kinetic energy of the system. The kinetic energy arises from particles hopping among adjacent lattice sites, whose effect is governed by energy scaling factor, $-J$. The second term corresponds to the potential. This depends on the strength of interactions between particles, controlled by the parameter, U. When $U = \infty$, the lattice is infinitely repulsive and two particles of opposite spin cannot hop over each other.

It has been shown [1] that the $U = \infty$ model can be effectively studied using an emergent Hamiltonian method, however, at finite U the absence of a simple boost operator makes the process difficult. We are currently studying this problem and expect that in an appropriate basis of quasi-particles this problem can be solved.

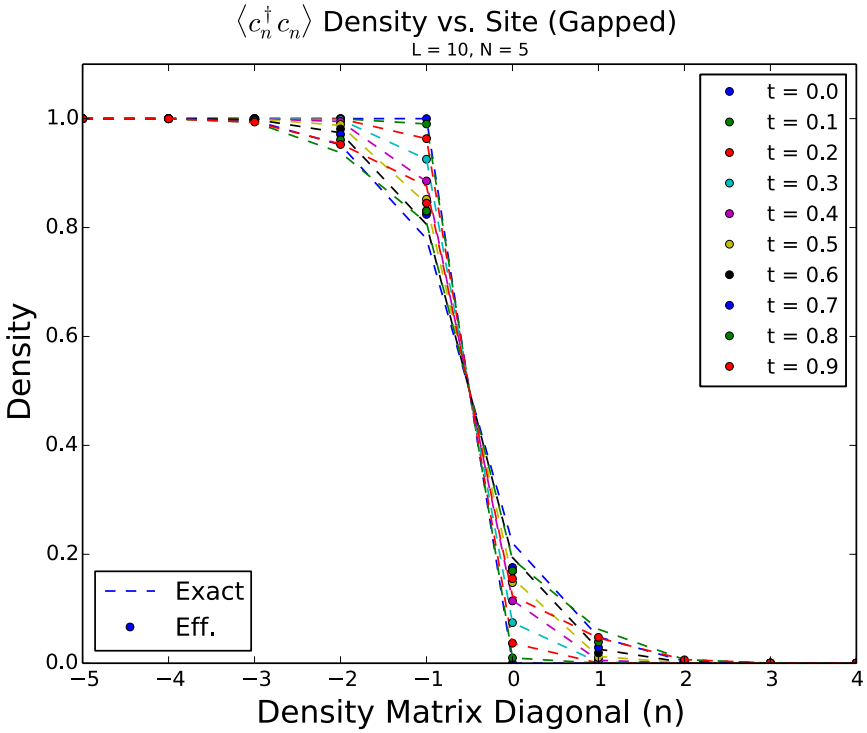

Figure 5.2: Occupancy distribution at various times for gapped t-V model, domain wall setup for $J = 1.0, V = 4.0$. Exact results are given by the dashed lines. Particles initially occupy the left half of lattice. Exhibits similar melting pattern as seen in the noninteracting domain wall and ungapped t-V model. In this case, however, the system exhibits diffusive transport along the lattice. The domain wall does not melt as quickly as in the previous case, below the critical point, $V/J = 2.0$. Particles flow into the right half of the lattice more slowly than in the ungapped case. In the plot, the occupancy distribution maintains its initial shape for much longer in the gapped model compared to the ungapped model.

Chapter 6

Discussion and Outlook

One-dimensional quantum systems driven far from equilibrium exhibit interesting behavior as they relax. These dynamics are not understood generally via standard statistical mechanical methods, as mentioned in Section 1.1. A particularly interesting element of the equilibration dynamics are the long-range correlations that develop seen in Figures 4.6 and 4.3. We start all systems in an eigenstate of an initial Hamiltonian. Consider the domain wall setup in Figure 1.1, consisting of noninteracting fermions at zero temperature in Section 4.1.1. This is an uncorrelated state. As the system evolves, however, the particles become entangled. We showed that infinite temperature systems still exhibit these power-law correlations, which we only expect in a low energy state. This suggests that thinking about these high-energy dynamical states as being equivalent to high temperature or disordered states is incorrect. It is important to note that temperature is an equilibrium quantity; it is not well-defined in these types of far from equilibrium setups. For nonzero temperature, states are described as mixed states. The emergent approach shows that even though these are mixed states of the emergent Hamiltonian, the special properties of the emergent Hamiltonian allow them to develop long-range correlations.

We hope to be able to extend the finite temperature results to interacting systems, and be able to study in more detail the differences between gapped and gapless systems directly using the emergent Hamiltonian. One might also use this approach to study entanglement entropy and other measures of coherence in experimentally realizable dynamical states.

Appendix A

Matrix Algebra

A.1 Eigenvectors and Eigenvalues

The material presented in this section is established in Sheldon Axler, "*Linear Algebra Done Right*", Chapter 5 [44]. Consider a square $n \times n$ matrix, M, and length n vector, v, given by,

$$M = \begin{bmatrix} a_{11} & a_{12} & \cdots & a_{1n} \\ a_{21} & a_{22} & \cdots & a_{2n} \\ \vdots & \vdots & \ddots & \vdots \\ a_{n1} & a_{n2} & \cdots & a_{nn} \end{bmatrix}, \qquad v = \begin{bmatrix} v_1 \\ \vdots \\ v_n \end{bmatrix}. \tag{A.1}$$

The product of an $n \times n$ matrix and a length n vector is another length n vector. Each entry of the resulting vector is the dot product of the vector with the corresponding matrix row. Multiplying M and v, we have

$$Mv = \begin{bmatrix} a_{11} & a_{12} & \cdots & a_{1n} \\ a_{21} & a_{22} & \cdots & a_{2n} \\ \vdots & \vdots & \ddots & \vdots \\ a_{n1} & a_{n2} & \cdots & a_{nn} \end{bmatrix} \begin{bmatrix} v_1 \\ \vdots \\ v_n \end{bmatrix} = \begin{bmatrix} a_{11}v_1 + a_{12}v_2 + \cdots + a_{1n}v_n \\ \vdots \\ a_{n1}v_1 + a_{n2}v_2 + \cdots + a_{nn}v_n \end{bmatrix}. \tag{A.2}$$

It is possible that the multiplication of a matrix M and vector v yields a multiple

of v. That is,

$$Mv = \lambda v \tag{A.3}$$

for some scalar λ. Note that λv is just v with each element multiplied by a factor of λ. In this case, we say that λ is an eigenvalue of matrix M and v is its corresponding eigenvector. An eigenvalue can have multiple associated eigenvectors. In fact, any scalar multiple of an eigenvector is also an eigenvector.

A.2 Bases

A vector space is a set of vectors that are well-defined under addition and scalar multiplication. A vector space must be commutative, associative, distributive, and contain an additive identity, additive inverse, and multiplicative identity for all vectors. For further information on vector spaces, see Axler "*Linear Algebra Done Right*", Chapter 1 [44].

Let V be an arbitrary vector space. Because V must have well-defined addition and scalar multiplication operations, a multiple of any vector in a V and the sum of any two vectors in V must also be in V. It follows that there exists a particular set of vectors in every space that span V. That is, every vector in V can be written as a linear combination of these vectors.

A basis of V is also a particular set of vectors in V that spans V. However, in addition to spanning V, all vectors in a basis must be linearly independent. This means no vector in the basis can be written as a linear combination of other elements in that set. So if a linearly independent set of vectors in V spans V, then the set forms a basis for V.

A.3 Orthogonality

An inner product on a vector space takes two vectors in the space to a number in the field over which the vector space is defined. The properties of an inner product are given in Axler "*Linear Algebra Done Right*", Section 6.A [44]. In this context, the inner product of two vectors, ϕ and ψ, is denoted $\langle\phi|\psi\rangle$. Two vectors are said to

be orthogonal if their inner product is 0. Two vectors are said to be orthonormal if they each have magnitude 1 and their inner product is 0 [44].

Every finite-dimensional vector space has an orthonormal basis [44]. Quantum states are written with respect to orthonormal bases. Every physical observable has a corresponding orthonormal basis [45]. Such bases allow us to easily represent states in terms of different physical quantities. For further reference, see Appendix B.

Appendix B

Hilbert Space

Hilbert space is a vector space in which quantum states and physical observables are represented. Quantum states are represented as vectors with respect to a particular basis. We may write

$$|\psi\rangle = [\alpha_1, \alpha_2, \ldots, \alpha_n]$$

to denote a quantum state with respect to some n-dimensional basis. For each j, entry α_j is the coefficient on the basis vector j.

Physical observables, such as energy or momentum, are given as operators on Hilbert space. These operators are represented as matrices with respect to some basis. These matrices are Hermitian. A matrix is Hermitian if it is equal to its conjugate transpose. Hermitian matrices have real eigenvalues [44]. This is expected, as measured values must be real.

B.1 Completeness Relation

In addition to the fundamental properties of a vector space (see Sheldon Axler's "*Linear Algebra Done Right*", Section 1.B [44]), Hilbert space is complete, meaning that every Cauchy sequence converges to a limit in Hilbert space. For information on Cauchy sequences, see Stephen Abbott's "*Understanding Analysis*", Chapter 6 [46].

Hilbert space also forms an inner product space, which is defined in Axler's "*Linear Algebra Done Right*", Section 6.A [44]. In this context, the inner product is written

$$\langle \phi | \psi \rangle = \int \phi^*(x)\psi(x)dx \tag{B.1}$$

for vectors ϕ and ψ.

Here I define the completeness relation as established in Shankar's "*Principles of Quantum Mechanics*", Section 1.6 [45]. The identity operator, $\mathcal{I}$, is written as a diagonal matrix consisting of 1's along the diagonal. Thus, for orthonormal states $|i\rangle, |j\rangle$, we have

$$\langle i|\mathcal{I}|j\rangle = \langle i|j\rangle = \delta_{ij}. \tag{B.2}$$

Let $\{|0\rangle, |1\rangle, \ldots, |n\rangle\}$ be an arbitrary orthonormal basis. Given state $|\psi\rangle$, we can expand in this basis as

$$|\psi\rangle = \sum_{i=1}^{n} |i\rangle\langle i|\psi\rangle \tag{B.3}$$

where $\mathcal{P}_i = |i\rangle\langle i|$ is called the projection operator. Since Equation B.3 is true for all states in Hilbert space, it follows that

$$\mathcal{I} = \sum_{i=1}^{n} |i\rangle\langle i| = \sum_{i=1}^{n} \mathcal{P}_i. \tag{B.4}$$

This is known as the completeness relation. Using this, we can easily represent any quantum state in terms of any particular basis.

B.2 Commutation Relations

In classical physics, all physical properties of a system can be known simultaneously. This is not true in general for quantum mechanics. The commutator of two observables describes to what precision both quantities can be known simultaneously. The commutator of two operators $\hat{A}$ and $\hat{B}$ is defined,

$$[\hat{A}, \hat{B}] = \hat{A}\hat{B} - \hat{B}\hat{A}. \tag{B.5}$$

If two operators commute, then they share eigenstates [44]. This means that their corresponding observables can be known simultaneously. For example, the commutator of position operator, $\hat{X}$, and momentum operator, $\hat{P}_x$, is

$$[\hat{X}, \hat{P}_x] = i\hbar. \tag{B.6}$$

So the position and momentum of a quantum particle cannot both be known with infinite precision. This gives rise to the Heisenberg uncertainty relation

$$\Delta x \Delta p_x \geq \frac{\hbar}{2}. \tag{B.7}$$

Commutation relations also appear in the Baker-Campbell-Hausdorff formula given by

$$\text{Exp}[X]\text{Exp}[Y] = \text{Exp}\left[X + Y + \frac{1}{2}[X, Y] + \frac{1}{12}\left([X, [X, Y]] + [Y, [Y, X]]\right) + \cdots\right]. \tag{B.8}$$

For further information on commutation relations, see David McIntyre's "*Quantum Mechanics: A Paradigms Approach*", Section 2.3 [7].

References

[1] L. Vidmar, D. Iyer, and M. Rigol, "Emergent eigenstate solution to quantum dynamics far from equilibrium," arXiv preprint arXiv:1512.05373 (2015).

[2] T. Kinoshita, T. Wenger, and D. S. Weiss, "A quantum newton's cradle," Nature, **440 7086**, 900 (2006).

[3] J. Lamers, "A pedagogical introduction to quantum integrability, with a view towards theoretical high-energy physics," arXiv preprint arXiv:1501.06805 (2015).

[4] H. M. Jaeger and A. J. Liu, "Far-From-Equilibrium Physics: An Overview," ArXiv e-prints (2010).

[5] R. Vasseur and J. E. Moore, "Nonequilibrium quantum dynamics and transport: from integrability to many-body localization," Journal of Statistical Mechanics: Theory and Experiment, **2016 6**, 064010 (2016).

[6] D. Schroeder, *An Introduction to Thermal Physics* (Addison Wesley, 2000).

[7] D. McIntyre, C. Manogue, J. Tate, and O. S. University, *Quantum Mechanics: A Paradigms Approach* (Pearson, 2012).

[8] A. Polkovnikov, K. Sengupta, A. Silva, and M. Vengalattore, "Colloquium: Nonequilibrium dynamics of closed interacting quantum systems," Reviews of Modern Physics, **83**, 863 (2011).

[9] J. M. Deutsch, "Quantum statistical mechanics in a closed system," Phys. Rev. A, **43**, 2046 (1991).

[10] M. Srednicki, "Chaos and quantum thermalization," Phys. Rev. E, **50**, 888 (1994).

[11] M. Rigol, V. Dunjko, and M. Olshanii, "Thermalization and its mechanism for generic isolated quantum systems," Nature, **452 7189**, 854 (2008).

[12] J. Eisert, M. Friesdorf, and C. Gogolin, "Quantum many-body systems out of equilibrium," Nature Physics, **11 2**, 124 (2015).

[13] L. D'Alessio, Y. Kafri, A. Polkovnikov, and M. Rigol, "From quantum chaos and eigenstate thermalization to statistical mechanics and thermodynamics," arXiv preprint arXiv:1509.06411 (2015).

[14] J.-S. Caux and J. Mossel, "Remarks on the notion of quantum integrability," Journal of Statistical Mechanics: Theory and Experiment, **2**, 02023 (2011).

[15] L. Vidmar and M. Rigol, "Generalized Gibbs ensemble in integrable lattice models," Journal of Statistical Mechanics: Theory and Experiment, **6**, 064007 (2016).

[16] J.-S. Caux and F. H. L. Essler, "Time Evolution of Local Observables After Quenching to an Integrable Model," Physical Review Letters, **110 25**, 257203 (2013).

[17] T. Langen, S. Erne, R. Geiger, B. Rauer, T. Schweigler, M. Kuhnert, W. Rohringer, I. E. Mazets, T. Gasenzer, and J. Schmiedmayer, "Experimental observation of a generalized gibbs ensemble," Science, **348 6231**, 207 (2015).

[18] J. Sirker, R. G. Pereira, and I. Affleck, "Diffusion and Ballistic Transport in One-Dimensional Quantum Systems," Physical Review Letters, **103 21**, 216602 (2009).

[19] X. Zotos, F. Naef, and P. Prelovsek, "Transport and conservation laws," Phys. Rev. B, **55**, 11029 (1997).

[20] I. Bloch, "Ultracold quantum gases in optical lattices," Nature Physics, **1 1**, 23 (2005).

[21] I. Bloch, J. Dalibard, and S. Nascimbene, "Quantum simulations with ultracold quantum gases," Nat Phys, **8 4**, 267 (2012).

[22] A. Kirilyuk, A. V. Kimel, and T. Rasing, "Ultrafast optical manipulation of magnetic order," Rev. Mod. Phys., **82**, 2731 (2010).

[23] C. Chin, R. Grimm, P. Julienne, and E. Tiesinga, "Feshbach resonances in ultracold gases," Rev. Mod. Phys., **82**, 1225 (2010).

[24] L.-M. Duan, E. Demler, and M. D. Lukin, "Controlling spin exchange interactions of ultracold atoms in optical lattices," Phys. Rev. Lett., **91**, 090402 (2003).

[25] A. Altland and B. D. Simons, *Condensed matter field theory* (Cambridge University Press, 2010).

[26] J. Taylor, *Classical Mechanics* (University Science Books, 2005).

[27] J. Millen and A. Xuereb, "Perspective on quantum thermodynamics," New Journal of Physics, **18 1**, 011002 (2016).

[28] R. Haydock, V. Heine, and M. J. Kelly, "Electronic structure based on the local atomic environment for tight-binding bands. II," Journal of Physics C Solid State Physics, **8**, 2591 (1975).

[29] C. M. Goringe, D. R. Bowler, and E. Hernández, "Tight-binding modelling of materials," Reports on Progress in Physics, **60**, 1447 (1997).

[30] F. Gleisberg, W. Wonneberger, U. Schlöder, and C. Zimmermann, "Noninteracting fermions in a one-dimensional harmonic atom trap: Exact one-particle properties at zero temperature," (2000).

[31] P. Vignolo and A. Minguzzi, "One-dimensional non-interacting fermions in harmonic confinement: equilibrium and dynamical properties," Journal of Physics B Atomic Molecular Physics, **34**, 4653 (2001).

[32] J. M. Luttinger, "An Exactly Soluble Model of a Many-Fermion System," Journal of Mathematical Physics, **4**, 1154 (1963).

[33] F. D. M. Haldane, "'luttinger liquid theory' of one-dimensional quantum fluids. i. properties of the luttinger model and their extension to the general 1d interacting spinless fermi gas," Journal of Physics C: Solid State Physics, **14 19**, 2585 (1981).

[34] D. C. Mattis and E. H. Lieb, "Exact Solution of a Many-Fermion System and Its Associated Boson Field," Journal of Mathematical Physics, **6**, 304 (1965).

[35] M. Karbach and G. Muller, "Introduction to the Bethe ansatz I," eprint arXiv:cond-mat/9809162 (1998).

[36] P. Jordan and E. Wigner, "Über das paulische äquivalenzverbot," Zeitschrift für Physik, **47 9**, 631 (1928).

[37] N. F. MOTT, "Metal-insulator transition," Rev. Mod. Phys., **40**, 677 (1968).

[38] R. Jördens, N. Strohmaier, K. Günter, H. Moritz, and T. Esslinger, "A Mott insulator of fermionic atoms in an optical lattice," **455**, 204 (2008).

[39] P. A. Lee, N. Nagaosa, and X.-G. Wen, "Doping a mott insulator: Physics of high-temperature superconductivity," Rev. Mod. Phys., **78**, 17 (2006).

[40] V. E. Korepin and I. Roditi, "Charge and spin separation in the 1D Hubbard model," eprint arXiv:cond-mat/0012266 (2000).

[41] M. A. Cazalilla, R. Citro, T. Giamarchi, E. Orignac, and M. Rigol, "One dimensional bosons: From condensed matter systems to ultracold gases," Rev. Mod. Phys., **83**, 1405 (2011).

[42] G. Gómez-Santos, "Generalized hard-core fermions in one dimension: An exactly solvable luttinger liquid," Phys. Rev. Lett., **70**, 3780 (1993).

[43] R. Orbach, "Linear antiferromagnetic chain with anisotropic coupling," Phys. Rev., **112**, 309 (1958).

[44] S. J. Axler, *Linear Algebra Done Right*, Undergraduate Texts in Mathematics (Springer, 1997).

[45] R. Shankar, *Principles of quantum mechanics* (Plenum, New York, NY, 1980).

[46] S. Abbott, *Understanding Analysis*, Undergraduate Texts in Mathematics (Springer, 2010).